Title
SEISMIC VISIBILITY OF FRACTURES

Authors
Pyrak-Nolte, L.J.
Myer, L.R.
Cook, N.G.W.

Publication Date
1987-05-01

Lawrence Berkeley Laboratory
UNIVERSITY OF CALIFORNIA

EARTH SCIENCES DIVISION

Presented at the 28th U.S. Symposium on Rock Mechanics,
Tucson, AZ, June 29–July 1, 1987

RECEIVED
LAWRENCE
BERKELEY LABORATORY
JUL 26 1988
LIBRARY AND
DOCUMENTS SECTION

Seismic Visibility of Fractures

L.J. Pyrak-Nolte, L.R. Myer, and N.G.W. Cook

May 1987

Prepared for the U.S. Department of Energy under Contract Number DE-AC03-76SF00098.

Seismic visibility of fractures

L.J. Pyrak-Nolte
Department of Material Science and Mineral Engineering, University of California, Berkeley, California

L.R. Myer
Earth Science Division, Lawrence Berkeley Laboratory, Berkeley, California

N.G.W. Cook
Department of Material Science and Mineral Engineering, University of California, Berkeley, California

ABSTRACT

Laboratory measurements of seismic travel times of compressional waves, propagated through both intact and naturally fractured specimens of quartz monzonite, were used to determine velocities of propagation. Velocities calculated from a quasi-static model were found to be too low compared to the measured velocities. A theoretical velocity is derived, based on the displacement discontinuity model of wave propagation across a fracture, which depends on the dynamic stiffness of the fracture and on frequency. Comparisons of the measured velocities and those computed from the theory agreed, and confirm the appropriatness of the displacement discontinuity model to simulate wave propagation across the fracture. From this model, changes in group time delay and signal amplitude occur at the fracture and are not distributed throughout the rock. These effects are a function of frequency and the stiffness of the fracture. This suggests that the use of seismic tomographic techniques would yield both the location and mechanical properties of discrete fractures.

INTRODUCTION

The seismic visibility of fractures is a central problem in the exploration of the earth's subsurface and monitoring of processes that occur therein. Whether for the recovery of oil, isolation of waste, or the study of active faults, knowledge of the location and properties of fractures is required for an understanding of the hydrologic and mechanical properties of rock masses.

In general, it is known that the presence of fractures will result in slower seismic velocities and smaller amplitudes than would be observed if no fractures were present. Based on these effects, several studies have shown the potential for using seismic tomography and vertical seismic profiling (VSP) techniques for the location and charaterization of fractures in a rock mass (Peterson et al., 1985; Wong et al.,1983; Crampin, 1985; Majer et al., 1987; and others). The observed effects of fractures on seismic wave amplitudes can be an order of magnitude greater than the effects on velocities (King et al., 1986). However, in the absence of an apprpriate theoretical basis for interpreting amplitude data in terms of fracture detection and characterization, the prevailing emphasis in field studies is on the effect of fractures on seismic velocities.

The effect of fractures on seismic wave velocities has generally been modeled by first developing expressions for the effective elastic moduli of the fractured rock mass and then relating these expressions to velocity through the elastodynamic equations. Various approaches have been taken. Kuster and Toksöz (1974) used a scattering formulation while O'Connell and Budiansky (1974) assume static loading conditions and employed the self-consistent approach to calculate effective moduli of a solid containing cracks or fractures small in extent in comparison to wavelength of the seismic wave. Assuming static loading conditions, Crampin (1981) derived effective anisotropic elastic moduli for rock masses with preferred orientation of such small cracks or fractures. White (1983) modeled relatively large fractures as two planes of infinite extent separated by Hertzian contacts and derived effective anisotropic moduli assuming static loading conditions. Seismic velocities derived from models such as those discussed above do not depend upon the frequency of the propagating waves. However, for dissipative media this frequency independence violates the principle of causality (White, 1983). In support of the theoretical argument for frequency dependent velocities, experimental results showing velocity dispersion have been obtained for rocks of widely varying porosities under different degrees of saturation over frequencies of 1 Hz to 1 MHz (Jones and Nur, 1983; Winkler, 1983; Spencer, 1981). Velocity dispersion in saturated rocks has been explained in terms of viscous interactions between the solid and the fluid (Spencer, 1981; Winkler, 1985 & 1986) while for dry rocks, a scattering mechanism has been proposed (Winkler, 1983).

An alternaitve model for describing the effect of fractures on both the velocity and the attenuation of seismic waves represents a single fracture as a displacement discontinuity. The basic premise of the model is that displacements of seismic waves are discontinuous across a fracture while stresses remain continuous. The general solution of Schoenberg (1980) can be used to show that a fracture will result in a frequency dependent group time delay as well as frequency dependent reflection and transmission coefficients. Here, this theory is used as a basis for the evaluation of a set of laboratory velocity measurements on samples containing single, through-going fractures, and an assessment of the influence of velocity dispersion on the detection of fractures in field applications.

EXPERIMENTAL PROCEDURE

Three pairs of quartz monzonite specimens (where a "pair" consists of one specimen with a natural fracture orthogonal to the long axis of the core and an adjacent intact specimen) were used to investigate the effect of single fractures on the amplitude and velocity of compressional waves. The specimens measured 52 mm diameter by 77 mm in length, and were subjected to stresses up to 85 MPa between steel pistons containing piezoelectric transducers. The waves were transmitted along the axis of the core. The natural frequency of each crystal was 1 MHz and the transmission crystals were pulsed with a 500 V spike of 0.3 μs duration at a repitition rate of 100 Hz. The arrival time of each pulse could be read to within 0.01 μs accuracy. Arrival times and transmitted wave amplitudes were recorded for each specimen under ambient conditions.

THEORY

The effects of a fracture on seismic wave propagation can be determined, theoretically, by representing the fracture by only a set of boundary conditions. These conditions state that the stresses across the fracture are continuous but the diplacements are not; the displacements are inversely proportional to the specific stiffness of the fracture. The essential equations for the magnitudes of the reflection (R) and transmission (T) coefficients and the phase, θ, of the transmission coefficent for a compressional wave normally incident upon a fracture (Schoenberg, 1980) are:

$$|R| = \left[\frac{\omega^2}{4(\kappa/Z)^2 + \omega^2} \right]^{1/2} \quad (1) \qquad |T| = \left[\frac{4(\kappa/Z)^2}{4(\kappa/Z)^2 + \omega^2} \right]^{1/2} \quad (2)$$

$$\theta = \tan^{-1} (\omega Z/2\kappa) \qquad (3)$$

where κ is the specific stiffness of the fracture, Z is the seismic impedance of the intact rock (velocity*density, $c^*\rho$), and ω is the frequency. The group time delay per fracture is given by:

$$t_g = \frac{d\theta}{d\omega} = \frac{2(\kappa/Z)}{4(\kappa/Z)^2 + \omega^2} \qquad (4)$$

All of these expressions (eqs. 1,2,3,4) depend on the ratio of stiffness of the fracture to the impedance of the intact rock and on the frequency. The group time delay, t_g, is the delay a pulse experiences on crossing a fracture. The group time delay has a maximum value at low frequencies and decreases with increasing frequency.

From the group time delay per fracture(eq. 4), an effective group velocity, c_{eff}, which depends on frequency and fracture stiffness, can be determined for a rock containing a fracture assuming no dispersion in the intact part of the rock or from multiple reflections. The effective group travel time, t_{eff}, for a wave passing through a rock with a fracture is

$$t_{eff} = \frac{1}{n\,c} + \frac{2(\kappa/Z)}{4(\kappa/Z)^2 + \omega^2} \qquad (5)$$

where c the seismic velocity of the intact rock and 1/n is the length of the path. Ignoring the interaction between fractures, n can be regarded as the number of fractures per unit length, as a first order approximation. The first term in eq. (5) is the time delay caused by the wave traveling through the intact rock, while the second frequency dependent term is the delay that arises because of the phase change across the fracture. The effective velocity, c_{eff}, which is equal to the length divided by t_{eff}, is

$$c_{eff} = \frac{c\,[\,1 + \{\omega/(2\kappa/Z)\}^2\,]}{1 + (\omega/(2\kappa/Z))^2 + (ncZ/2\kappa)} \qquad (6)$$

Theoretical curves of c_{eff} as functions of frequency are shown in Fig. 1, for several values of κ/Z. A constant intact rock impedance (c=5600 m/s, ρ=2600 kg/m^3) is assumed and 1/n is set to 0.077 m. In accordance with eq. (4), κ/Z determines the behavior of the effective velocity as a function of frequency. From Fig 1., when $\omega < 0.3(2\kappa/Z)$, the group time delay is large, yielding a low velocity. For $\omega > 30\,(2\kappa/Z)$, the group time delay is very small, so the effective velocity approaches the velocity assumed for the intact rock. In the transition region, $0.3\,(2\kappa/Z) < \omega < 30\,(2\kappa/Z)$, there is a rapid decrease in the group time delay resulting in a rapid increase in effective velocity. The initiation of this transition region occurs at lower frequencies for fractures with low stiffness ($\omega=2\pi \times 10^2$, $\kappa/Z=10^3$) and higher frequencies for stiff fractures ($\omega=2\pi \times 10^4$, $\kappa/Z=10^5$). Interestingly, this difference in the initiation frequency results in a transition region where, for a given frequency, a fracture of high stiffness will result in a lower effective velocity than a fracture

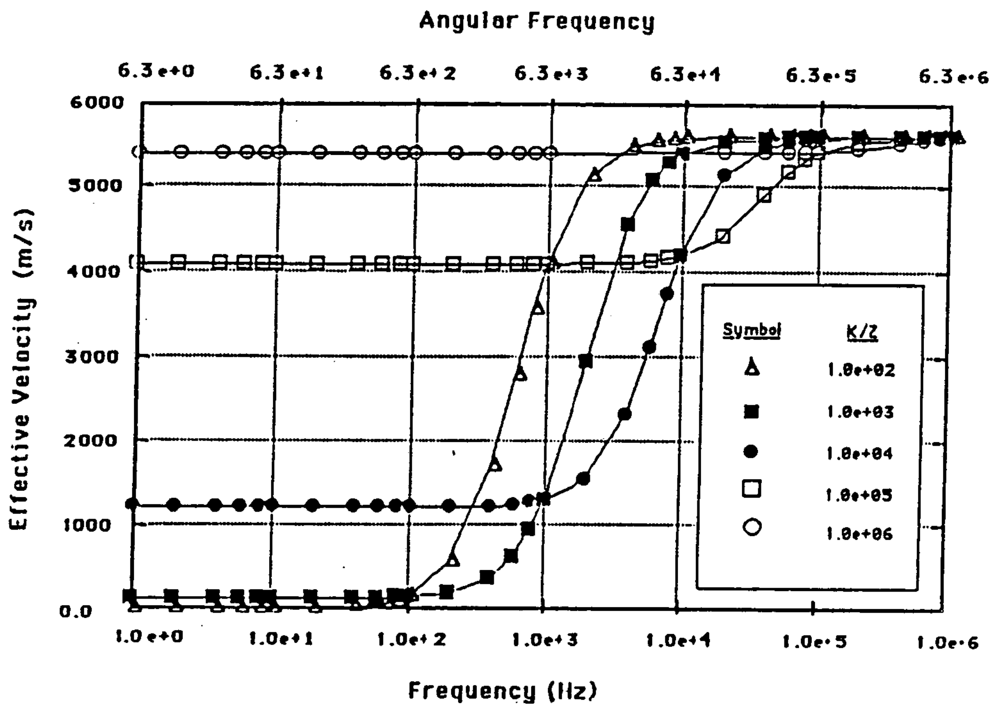

Figure 1. Curves of theoretical effective velocity as a function of stress for several values of κ/Z and a fracture spacing of 0.077 m.

of lower stiffness. The frequency region $\omega > 30\ (2\kappa/Z)$, where the effective velocity for the fracture approaches the velocity of the intact rock, corresponds to the range of frequencies where the transmission coefficient is a minimum and the reflection coefficient is a maximum. In this region, more information about the fracture is contained in the transmission or reflection amplitudes than in the travel time measurements.

Assuming that an equivalent effective dynamic modulus (uniaxial strain or plane wave modulus), D_{eff}, can be determined from $c_{eff} = \sqrt{D_{eff}/\rho}$. The effective dynamic modulus is

$$D_{eff} = D \left(\frac{1 + \{\omega/(2\kappa/Z)\}^2}{1 + (\omega/(2\kappa/Z))^2 + (nD/2\kappa)} \right)^2 \qquad (7)$$

where D is the dynamic modulus of the intact rock. Note that the frequency dependent group time delay results in a a frequency dependent effective dynamic modulus, D_{eff}.

In general, the velocity of propagation for plane compressional waves through a material depends upon the uniaxial strain elastic modulus of that material. A rock containing fractures will have a lower effective modulus than a rock containing no fractures. For a rock containing fractures, a quasi-static effective modulus, E'_{eff}, can be derived. To begin with

$$E'_{eff} = \sigma / \varepsilon_{eff} \quad , \qquad (8)$$

where σ is the stress, and ε_{eff} is the effective strain. The effective strain for a rock with fractures is defined as:

$$\epsilon_{eff} = (\sigma/E'_s) + (n\sigma/\kappa_s) \qquad (9)$$

where E'_s is the static uniaxial strain modulus of the intact rock, and κ_s the static uniaxial strain specific stiffness of the fracture. The first term in equation (9) is the strain in the intact rock for an applied stress, while the second term represents the additional strain due to the presence of the fracture. Substituting equation (9) into (8), and rearranging, results in the following equation for a quasi-static effective modulus:

$$E'_{eff} = E'_s \frac{1}{1 + (nE'_s/\kappa_s)} \qquad (10)$$

From the velocity equation, $c_{qs} = \sqrt{E'_{eff}/\rho}$, an effective quasi-static velocity can be found:

$$c_{qs} = c \sqrt{\frac{1}{1 + (nE'_s/\kappa)}} \qquad (11)$$

To lowest order approximation, the expression for the quasi-static effective velocity (eq. 11) is equivalent to the expression for the dynamic effective velocity (eq. 6) for the special case of $\omega \rightarrow 0$. However, if the seismic frequency increases, the group time delay decreases (eq. 4) and the value of the dynamic effective vleocity also increases.

RESULTS

The theory for wave propagation across a fracture dictates that a change in amplitude and group time delay occurs when the wave crosses the fracture, and both of these effects are in fact observed in the data. By comparing the complete received compressional wave signals of the intact specimen E35 (Fig. 2a) to that of the fractured specimen E35 (Fig. 2b), both subjected to a stress of 1.4 MPa, a reduction in amplitude and high frequency content of the signal, as well as, an increase in travel time for the fractured rock specimen are observed. Though the difference in travel times between the intact and fractured specimen data, is very small (0.37 μs), the difference in amplitude is quite large. These observations are consistent with the group time delay and the transmission behavior determined from the displacement discontinuity model, which predicts a small group time delay and a reduction in transmission at high frequencies.

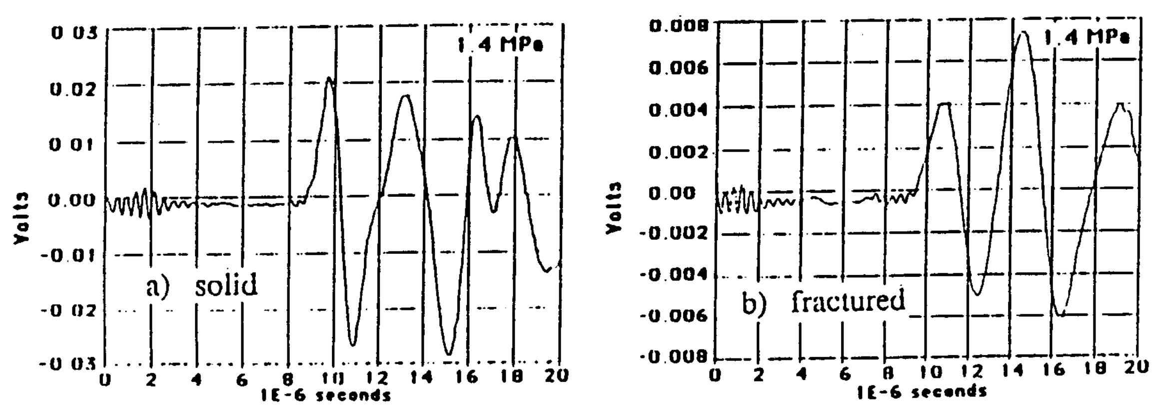

Figure 2. Complete received compressional wave signal for a) solid specimen E35 and b) fractured specimen E35 for a stress of 1.4 MPa.

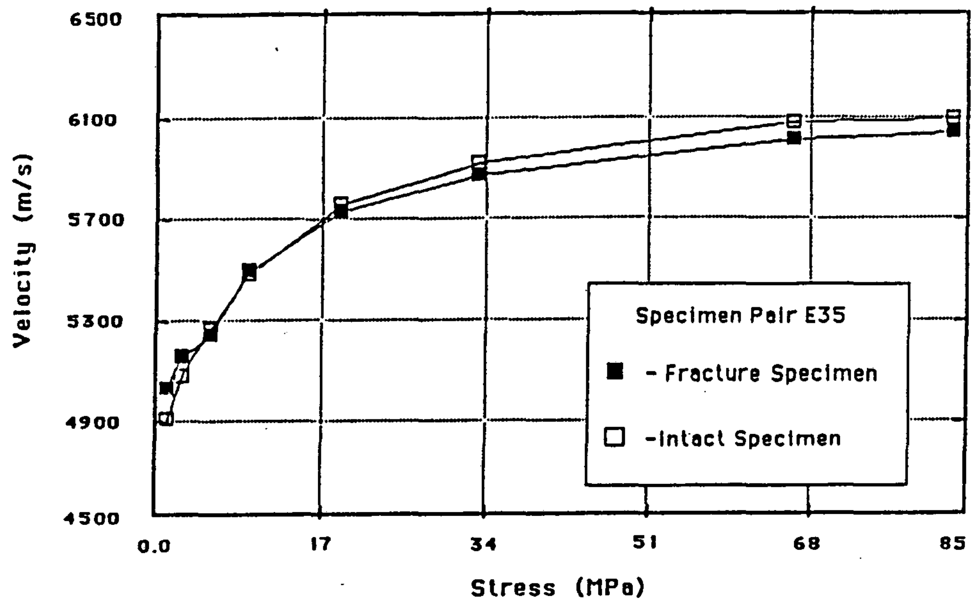

Figure 3. Velocities as a function of stress calculated from measured travel times for specimen pair E35.

For all the specimens pairs, velocities were calculated from measured travel times. For both the fractured and intact specimens, velocity was found to increase with increasing stress. The velocity data (Fig 3) for specimen pair E35, are representative of the trends observed in the other specimen pairs. The small difference in velocity between the intact specimen and the fractured specimen reflect the small differences in measured travel times for the two specimens.

A frequency dependent velocity (eq. 6) was calculated to compare with the theoretical effective velocity curves (Fig. 1). Fig. 4 is a graph of the effective velocity (equation 6) as a function of frequency, for fractured specimen E35, calculated from the measured dynamic stiffness of the fracture assuming a constant intact rock velocity of 5600 m/s and a length of 0.077 m. The dynamic stiffnesses for selected stresses (Table 1) were determined from the seismic results by curve matching (Pyrak-Nolte, 1987a). The results exhibit the same trends in behavior predicted by the theoretical effective velocity curves (Fig. 1). At some frequencies, the effective velocity is higher for lower values of fracture stiffness than for higher values of fracture stiffness. At high frequencies, all the curves of effective velocity approached an asymptote of 5600 m/s which was the assumed value of the intact rock velocity. At these high frequencies, the effect of the fracture on wave velocites is almost erased, but the effect of the fracture on the amplitude of the transmitted wave is very apparent (Fig. 2).

Table 1. Static and Dynamic Specific Stiffnesses for Fractured Specimen E35 for Selected Stresses

Stress (MPa)	Static Stiffness ($\times 10^{12}$ Pa/m)	Dynamic Stiffness ($\times 10^{12}$ Pa/m)
2.9	1.0	4.5
10.0	2.2	8.0
33.0	3.3	25.0

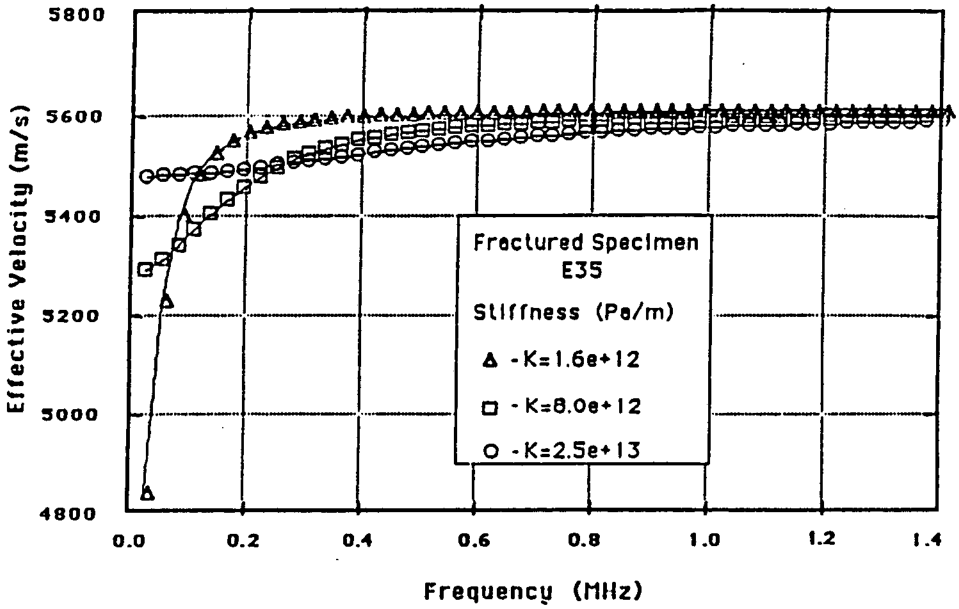

Figure 4. Effective velocity as a function of frequency for fractured specimen E35 calculated from measured values of stiffness, assuming the velocity of the intact rock to be 5600 m/s. (Based on equation 6)

In reality, the effective velocity of the intact rock varies with stress. Fig. 5 shows graphs of effective velocities as a function of frequency for fractured specimen E35 based on the measured dynamic stiffnesses and the measured, stress dependent velocities of intact specimen E35. Each effective velocity curve approached an asymptote equal to the velocity in the intact rock corresponding to that stress. No crossover in effective velocity with change in stiffness (stress) is observed because of the overriding effect of the stress dependent velocity of the intact rock.

The measured velocities were compared to the frequency dependent effective velocities

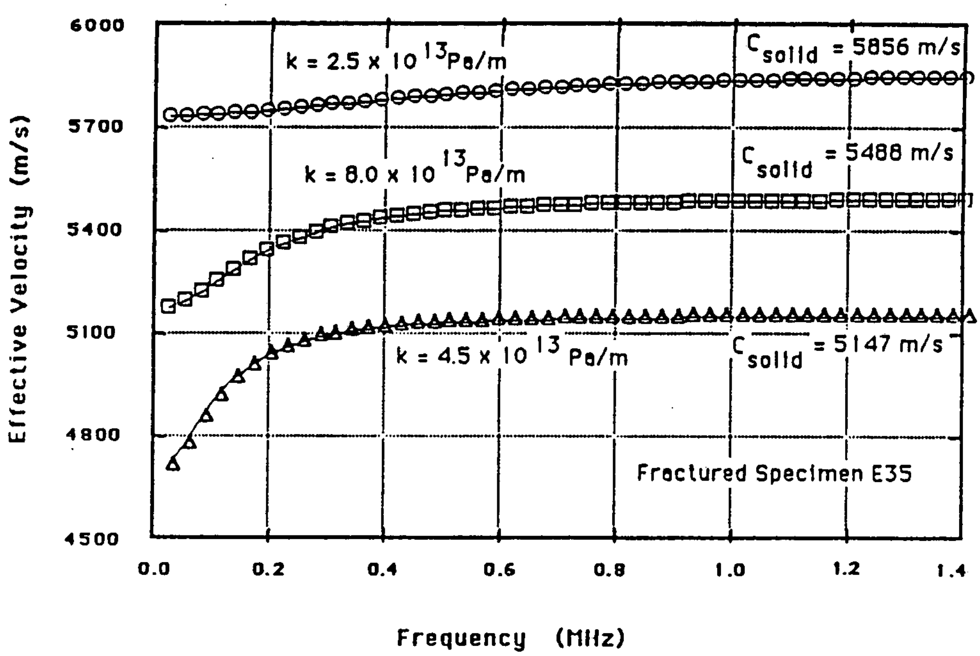

Figure 5. From equation 6, effective velocity as a function of frequency for fractured specimen E35 calculated from values of measured dynamic stiffness and measured intact rock velocities, c_{solid}.

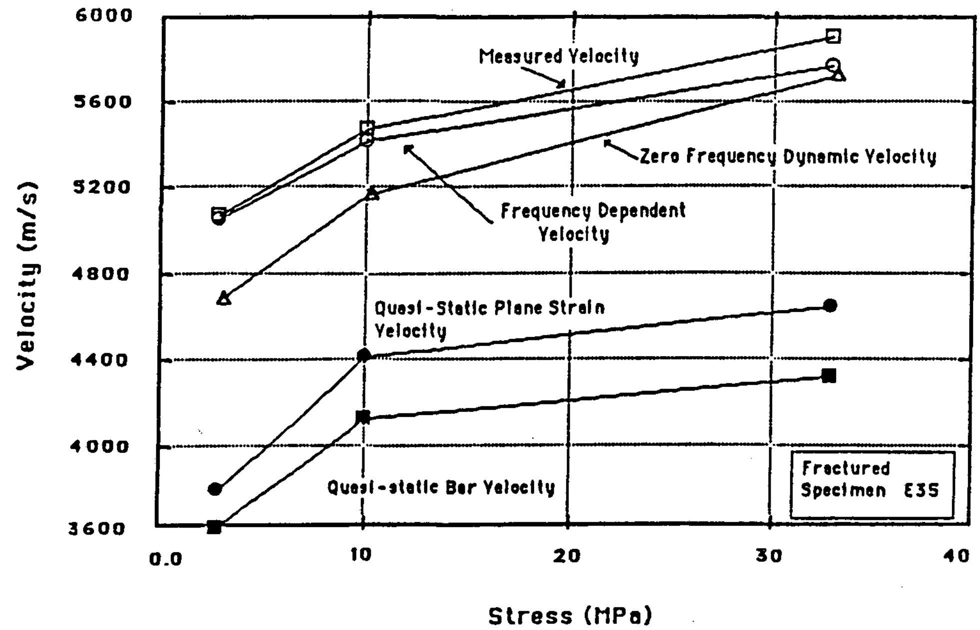

Figure 6. Velocity as a function of stress for fractured specimen E35 from i) frequency dependent velocity, ii) special case of the frequency dependent model of $\omega=0$, iii) quasi-static bar velocity, iv) quasi-static uniaxial strain or plane wave velocity, and v) measured velocity.

(eq. 6) and the zero frequency dynamic velocities at different stresses. The value of the frequency dependent effective velocity was calculated for the frequency corresponding to the maximum spectral amplitude. The frequency dependent effective velocities (eq. 6) fit the measured values of velocities well (Fig. 6). The zero frequency dynamic effective velocities are lower than the measured data and demonstrates the effect of frequency on velocity. The good fit between the measured velocities and the frequency dependent theoretical velocities confirms not only the frequency dependence of the effective velocity, but also the appropriateness of the displacement discontinuity model to simulate the effect of fractures on wave propagation.

Finally, measured values of the static specific fracture stiffness (Pyrak-Nolte, 1987b) made under uniaxial stress conditions, were used to deteremine an effective bar velocity assuming a Young's modulus for the intact rock of 60 GPa (Cook & Myer, 1981) and a density of 2600 kg/m^3. A quasi-static effective uniaxial strain or plane wave velocity was calculated by multipling the Young's modulus by $\{(1-v)/[(1-2v)(1+v)]\}$, assuming a Poission's ratio, v=0.25. Both the quasi-static effective bar velocity and the quasi-static effective plane wave velocity are much lower in value than the measured data (Fig.6). In part, this occurs because the frequency dependence of the group time delay is not taken into account in the quasi-static effective modulus approach, and in part, because dynamic moduli of intact rock are greater than static moduli (Jaeger & Cook, 1979: 188).

DISCUSSION

A simple compliance model (quasi-static) cannot predict either the frequency dependence of the group time delay nor the strong frequency dependent effect of fractures on the amplitudes of transmitted and reflected pulses. The displacement discontinuity model of wave propagation across a fracture, on the other hand, not only predicts the frequency dependence of the group time delay and the amplitude, but also is able to match the measured velocity data quite well. From this model, we find that the effects on amplitude and phase are particularly strong when the frequency of the seismic waves is of the order of the ratio between the stiffness of the fracture and the seismic impedance of the rock, ($\omega \geq K/Z$) or more. On the other hand, changes in travel time, in terms of group delay, are a maximum at low frequency and decrease with increasing frequency.

The seismic travel times from low frequency surveys can only yield effective velocities for bulk rock. Although high frequency data does not yield the correct effective moduli (unless the frequency dependent nature of the group time delay is taken into account) it does include changes in phase and amplitude caused by the fractures. Because these high frequency effects occur at the fracture and are not distributed throughout the rock, fractures could be detectable in borehole seismic tomography by examining not only travel times, but by also using amplitude and phase information.

Because the current investigation was performed using very high frequecnies compared to those used in the field, it is necessary to asses their applicability to real conditions. For example, a typical change in velocity, caused by the prescence of fractures, that is measured in the field at conventional seismic frequencies is five percent. Using either the quasi-static or low frequency models, the following relationships between the stiffness, κ, and the number of fractures per length, n, would maintain this five percent change in velocity:

n=	0.01	0.1	1	10	fractures/meter
κ=	10^{10}	10^{11}	10^{12}	10^{13}	Pa/m.

From equations (1) & (2), $|R| = 0.45$ and $|T| = 0.9$ when $[\omega/(\kappa/Z)] = 1.0$, so that frequencies at which fractures with the above stiffness could be located individually would be:

ω=	625	6250	62500	625000	cycles/sec
Hz=	100	1000	10k	100K	Hertz

Therefore, if a frequency of 100 Hz is used, a fracture with a stiffness of $\kappa = 10^{10}$ Pa/m, could be detected by virtue of its effect on reflected or transmitted amplitudes. Whereas, a frequency of 100 kHz would be required to detect of fractures with a stiffness of 10^{13} Pa/m.

The above analysis has been applied only for P-waves, normally incident on the fracture. However, the theory is applicable to more complicated situations of compressional or shear waves incident at all angles. It appears that if transmission coefficients could be measured, such as by cross-hole seismic tomography, in addition to changes in velocity, then fractures could be located in situ and their mechanical stiffness determined. The mechanical stiffness of fractures appears to bear a rank correltaion with hydrualic conductivity (Pyrak-Nolte, 1987b).

CONCLUSION

The displacement discontinuity theory shows that time delays and reductions of signal amplitude occur at the fracture and are not distributed throughout the whole rock as implied by effective modulus theory, so that seismic tomographic techniques could yield the location and stiffness characteristics of discrete fractures.

ACKNOWLEDGEMENTS

This work was supported in part by National Science Foundation grant CEE-8300531, in part by Office of Radioactive Waste Management through the Office of Geologic Repositories, and in part by Director of Basic Energy Sciences, Division of Engineering, Mathematics and Geosciences of the United States Department of Energy, contract number DE-AOC3-76SF00098.

References

Cook, N.G.W. & L.R. Myer. 1981. Thermo-mechanical studies on granite in Stripa, Sweden. In P. Hoffmann (ed.), Technology of high level nuclear waste disposal, p.87-99. DOE/TIC-4621 vol 1. Technical Information Center, Department of Energy.

Crampin, S. 1981. A review of wave motion in anisotropic and cracked elastic media. Wave Motion. 3:343-391.

Crampin, S. & S. Peacock. 1985. Shear-wave vibrator signals in transversely isotropic shale. Geophysics, 50:8:1285-1293.

Jaeger, J.C. & N.G.W. Cook. 1979. Fundamentals of rock mechanics. London. Chapman and Hall.

Jones, T. & A. Nur. 1983. Velocity and attenuation in sandstone at elevated temperatures and pressures. Geophys. Res. Let. 10:2:140-143.

King, M.S., Myer, L.R. & J.J. Rezowalli. 1986. Experimental studies of elastic-wave propagation in a columnar-jointed rock mass. Geophys. Prosp. 34:8:1185-1199.

Kuster, G.T. & M.N. Tosköz. 1974. Velocity and attenuation of seismic waves in two-phase media: Part I. Theorectical formulations. Geophysics. 39:9:587-606.

Majer, E.L., Mc Evilly, T.V., Eastwood, F.S. & L.R. Myer. 1987. Fracture detection using P- and S-wave VSP at the Geysers geothermal field. Accepted for publication in Geophysics.

O'Connell, R.J. & B. Budiansky. 1974. Seismic velocities in dry and saturated cracked rock. Jour. Geophys. Res. 79:35:5412-5426.

Peterson, J.F., Paulsson. B.N.P. & T.V. Mc Evilly. 1985. Application of algebraic reconstruction techniques to crosshole seismic data. Geophysics. 50:10:1566-1580.

Pyrak-Nolte, L.J. & N.G.W. Cook. 1987a. Effects of stresses, pore fluids and temperatures on the velocities and attenuation of seismic pulses. Final report to the National Science Foundation, in preparation.

Pyrak-Nolte, L.J., Myer, L.R., Cook, N.G.W. & P.A. Witherspoon. 1987b. Hydraulic and mechanical properties of natural fractures in low permeability rock. To appear in the proceeding for the Sixth International Rock Mechanics Symposium Montreal, Canada.

Schoenberg, M. 1980. Elastic wave behavior across linear slip interfaces. Jour. Acous. Soc. Amer. 68:5:1516-1521.

Spencer, J.W. 1981. Stress relaxations at low frequencies in fluid saturated rocks: attenuation and modulus dispersion. Jour. Geophys. Res. 86:B3:1803-1812.

White, J.E. 1983. Underground Sound, p. 83-138. Amsterdam: Elsevier.

Winkler, K.W. 1983. Frequency dependent ultrasonic properties of high-porosity sandstones. Jour. Geophys. Res. 88:B11:9493-9499.

Winkler, K.W. 1985. Dispersion analysis of velocity and attenuation in Berea Sandstone. Jour. Geophys. Res. 90:B8:6793-6800.

Wong, J., Hurley, P. & G.F. West. 1983. Crosshole seismology and seismic imagining in crystalline rocks. Geophys. Res. Let. 10:8:686-689.

LAWRENCE BERKELEY LABORATORY
OFFICE FOR PLANNING AND DEVELOPMENT
UNIVERSITY OF CALIFORNIA
BERKELEY, CALIFORNIA 94720